

# Application of PIXE and PIGE under variable ion beam incident angle to several fields of archaeometry<sup>†</sup>

G. Weber,<sup>1,3\*</sup> L. Martinot,<sup>1</sup> D. Strivay,<sup>1,3</sup> H. P. Garnir<sup>1,3</sup> and P. George<sup>2</sup>

<sup>1</sup> IPNAS, University of Liège, Sart-Tilman B15, 4000 Liège, Belgium

<sup>2</sup> Treasury House of Liège Cathedral, Rue Bonne Fortune 6, 4000 Liège, Belgium

<sup>3</sup> Centre Européen d'Archéométrie (CEA)

Received 16 September 2004; Accepted 4 January 2005

For several years, the specific features of PIXE and PIGE have made them very attractive in the field of archaeometry. Among them, non-destructivity is one of the most important. The possibility of working under atmospheric pressure is also important because of the very different shapes and sizes of the artefacts concerned. However, these ion beam techniques suffer from the same disadvantage: the information coming from x-rays or  $\gamma$ -rays produced at different places along the charged particle path is integrated. That prevents one from taking into account the possible element concentration gradients due to multi-layered systems or diffusion processes. This paper presents several applications of PIXE and PIGE applied under variable ion beam incident angle. PIGE has been mainly used for studying ancient glass items or glass windows in order to detect or evaluate the glass corrosion process. The examples given for PIGE deal with Roman and Merovingian glass objects and cathedral glass windows and PIXE applications concern studies for resolving the multilayered structure of easel paintings. The set-up allowing one to perform the measurements should be very stable, the rotation axis should pass through the beam axis and the detector should follow the sample movement. Copyright © 2005 John Wiley & Sons, Ltd.

## INTRODUCTION

A real problem is encountered when applying PIXE and PIGE, two very important methods in the field of archaeometry,<sup>1–3</sup> namely that for one incident energy and under fixed incidence, it is not possible to distinguish between spectroscopic information coming from different depths in a multi-layered sample. This paper presents three typical examples chosen among many others where, by tilting the sample, it is possible to give some answer to the problem mentioned above. The information obtained can be very useful in the art field. In painting, it often shows how the artist worked. It is also able to detect fakes or restorations by detecting, for example, non-chronological sets of pigment layers. The detection of corrosion having taken place without showing visual symptoms can help to guide the curator in choosing the conservation conditions.

## EXPERIMENTAL

The experimental atmospheric PIXE–PIGE set up at IPNAS, Liège, has been described elsewhere<sup>4,5</sup> but its main specific feature is the possibility of rotating the sample around an axis passing through the beam path. This sample holder

is specially designed to allow the x-ray detector to follow the sample movement. It is important in the case of PIXE measurements where x-rays, produced at a certain depth, are partially absorbed by the sample material on their way towards the sample surface. This absorption depends on the depth where the x-rays or  $\gamma$ -rays are produced and on the angle between the beam direction and the detector axis. In order to reduce the number of parameters concerned, this angle should be kept constant. For PIGE, this problem is negligible because of the weak absorption of the  $\gamma$ -rays by thicknesses corresponding to the range 2–3 MeV protons in the material considered. The proton beam is extracted in air using a thin nickel foil (2.5  $\mu$ m). This metal was chosen because of its good thermal strength and because it does not produce  $\gamma$ -rays under proton bombardment. The particle beam is monitored by counting the protons scattered by a gold layer (50 nm) deposited on a polycarbonate backing, which interrupts the beam at a 2 Hz frequency.

## PRINCIPLE OF VARIABLE INCIDENT ANGLE METHOD

The principle of the method is the same for both PIXE and PIGE. It consists in a rotation of the sample around an axis passing through the beam path. Rotating the sample and observing that the beam spot did not move checked this condition. Figure 1 shows the case of a simplified sample composed of two layers.

By rotating the sample, one changes the relative path-length in the two layers, leading to an enhancement of the signal corresponding to the superficial layer and reducing the signal corresponding to the inner layer.

\*Correspondence to: G. Weber, IPNAS, University of Liège, Sart-Tilman B15, 4000 Liège, Belgium. E-mail: g.weber@ulg.ac.be

<sup>†</sup>Presented at 10th International Conference on Particle Induced X-ray Emission and its Analytical Applications, PIXE 2004, Portoroz, Slovenia, 4–8 June 2004.

Contract/grant sponsor: Institut Universitaire des Sciences Nucléaires.

Contract/grant sponsor: French Belgium Community (ARC).

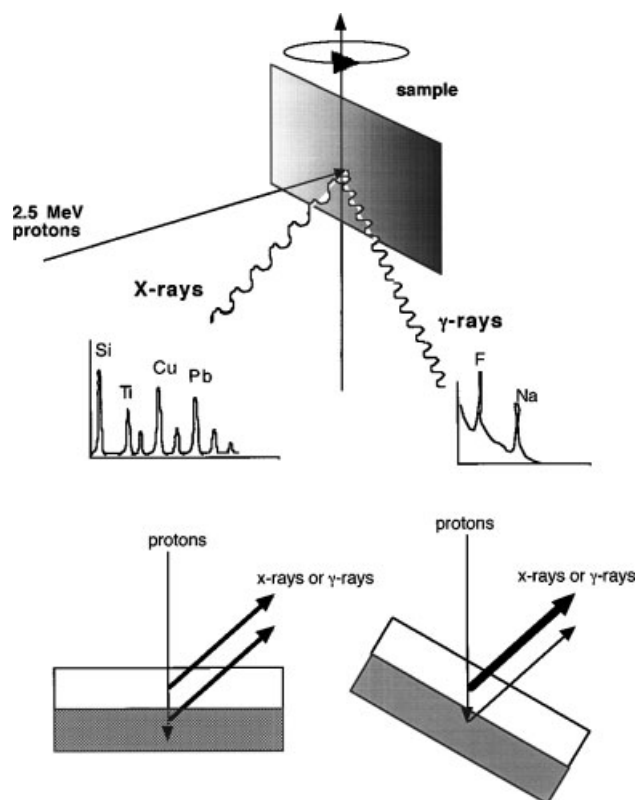


**Figure 1.** Experimental set-up and principle of the variable incident beam angle. As an example, the range of 2.5 MeV protons in glass is about 60  $\mu\text{m}$ .

As we will see further, the phenomenon is easier to handle in PIGE than in PIXE because of the weaker absorption of  $\gamma$ -rays compared with x-rays. The results obtained in PIXE will be more qualitative than in PIGE. Some surface effect arises when the incident angle is beyond 70°. As the detection angle is different from zero, at large incident angle the surface irregularities play a more and more important role by perturbing the thickness crossed by the x-rays on their way to the detector. This is the reason why, mainly in PIXE, some dispersion of experimental values arises. The use of several proton energies helps in this context because it allows the use of only small angles where the surface problems are negligible.

## RESULTS AND DISCUSSION

### Determination of the depth reached by silver yellow on a stained glass window (PIXE)

Gold aspect in stained glass windows has generally been obtained by firing transparent glass on to which silver nitrate mixed with medium has been painted.<sup>6</sup> The result is a gold-coloured zone due to a thin layer of metallic silver at some distance from the surface. It is interesting to know that distance because silver yellow is often considered a protective layer against the corrosion process. In Fig. 2, by comparing the theoretical evolution of the Ag x-ray detected as a function of the incident angle with the experimental values, one can estimate the distance mentioned above as about 1.5  $\mu\text{m}$ . The theoretical values were calculated by taking into account the variation of the incident angle and

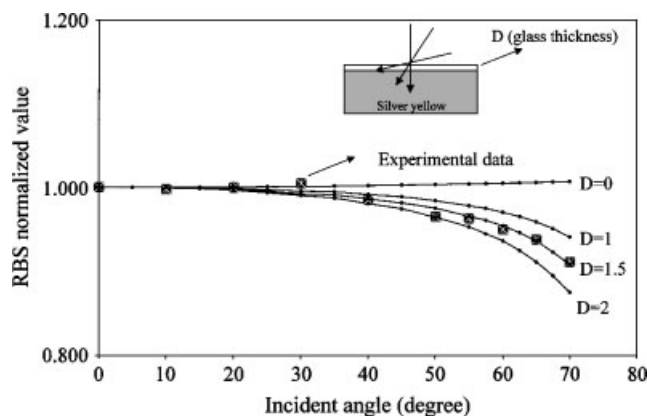


**Figure 2.** Determination of the depth reached by the silver yellow stain in the glass window.

the proton range in glass. The preliminary determination of the glass composition in major elements is essential for computing the proton stopping power<sup>7</sup> and the x-ray attenuation coefficient.<sup>8</sup> The x-ray yield cross-section for K and L x-rays, as a function of the proton energy, were obtained from Refs 9 and 10, respectively.

### Determination of the stratigraphy present on a Byzantine icon

An icon belonging to the Treasure House of Liège Cathedral was investigated. Among the different pigments identified by a normal incident beam, a red one was particularly difficult to explain. In this red area, we found several elements corresponding to a lake (Al, Si, Ca and Fe), three elements indicating the presence of a metallic layer (Au, Ag and Cu) and also Zn. The presence of the last element is very surprising because white zinc appears to date only from the end of the 18th century.<sup>11</sup> Fig. 3 shows the results obtained by tilting the sample. The curves are simply the result of the linking of the experimental results relating to each element. The evolution of the signal relating to Fe, Au and Zn allows the stratigraphy reported on the graph to be proposed. The Fe  $K\alpha$  line is continuously increasing, which proves its position in first place at the surface. The Au  $L\beta$  line increases first, but from 55° its behaviour changes and a decrease takes place, because around 55° tilting the proton beam leaves the progressively deepest side of the metallic

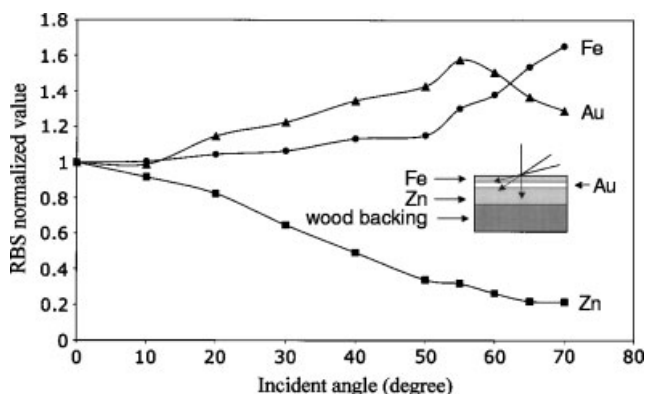


**Figure 3.** Evolution of Fe, Au and Zn as a function of the proton beam incident angle.

layer. The choice of the Au  $L\beta$  line is due to the interference between the Au  $L\alpha$  line and the Zn  $K\beta$  line. Then, one can propose the second place for this layer just under the red lake. For Zn, the constant decreasing of the Zn  $K\alpha$  line indicates the third position for this element under red lake and gold-silver alloy. An attempt to explain the presence of a metallic layer (foil or metal powder + binder) under the red lake could be the use of the 'mordant' or 'sgraffito' gilding technique for embellishing Jesus's robe by imitating gold embroidery.<sup>12</sup>

The reason for the presence of zinc in the pictorial layer should then be found elsewhere. This icon was restored by Mr J. van de Veken (Brussels) in 1935. From the content of a letter sent by Mr van de Veken to J. Puraye,<sup>13</sup> it has been possible to resolve the problem of the zinc present everywhere on the pictorial layer. Originally, the latter was applied on a parchment, which was then glued on a cedar backing.

As the wood dramatically deteriorated, mainly by woodworm attack it was decided to transpose the pictorial layer to a new backing. First, the icon was stuck on several paper foils with a glue likely to be easily dissolved later. A rigid structure was then obtained (pigments + parchment + paper), allowing the next operation, which consisted in removing mechanically the deteriorated wood. A new backing was prepared by covering a wood panel surface with gesso, which is composed of rabbit skin glue (RSG), zinc white and gypsum. The pictorial layer was then laid to the new panel and the paper removed by dissolving the glue from the top side. It is then clear that the origin of Zn has to be found in the gesso composition.

This study shows that the use of PIXE under normal incidence could lead to misinterpretation of the presence of some pigments in a multi-layered system.

### Analysis of weathering glasses (PIGE)

Corrosion of ancient glass objects is generally due to the leaching of Na when the glass surface is in contact with water. It is then of interest to measure the Na concentration gradient within the first 50  $\mu\text{m}$  of the glass thickness.

The cross-section of the reaction  $^{23}\text{Na}(p,p'\gamma)^{23}\text{Na}$  is large and well known<sup>14</sup> between 1 and 4 MeV protons. As the  $\gamma$ -rays produced (0.44 and 1.63 MeV) are not much absorbed, it is possible to measure the Na concentration gradient up to 30–90  $\mu\text{m}$  by using PIGE under variable incident angle. Figure 4 shows an example of scanning obtained with four different incident angles,  $\Phi_0 = 0$ ,  $\Phi_1$ ,  $\Phi_2$  and  $\Phi_3$ . Assuming that the proton range in glass is constant, each result  $S_i$  ( $i = 0-3$ ) gives information about the depth reached perpendicular to the sample surface. These  $S_i$  are in fact a set of four equations in four unknowns  $C_1$ . Knowing the stopping power of the proton in glass and the integrated cross-section of the nuclear reaction,<sup>14</sup> it is easy, by a simple matrix inversion, to obtain the Na concentrations in each zone. Note that on Fig. 4, only four angles have been used. It is clear that if one multiplies the number of incident angles, the differential thickness of the analysed layers decreases and the precision obtained increases.

Figure 5 shows that, as expected, for modern glass there is no variation of the Na concentration. Two incident energies

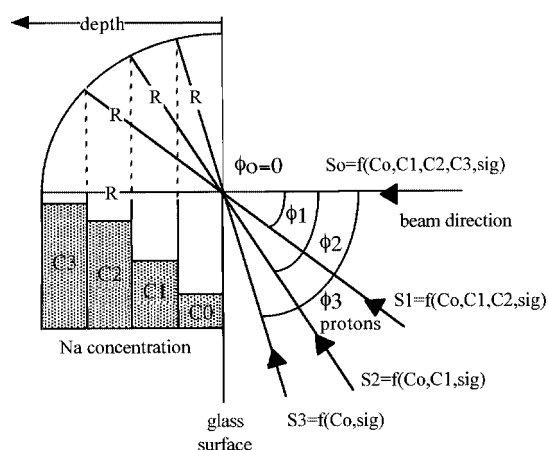


Figure 4. Principle of the PIGE under variable incident angle.

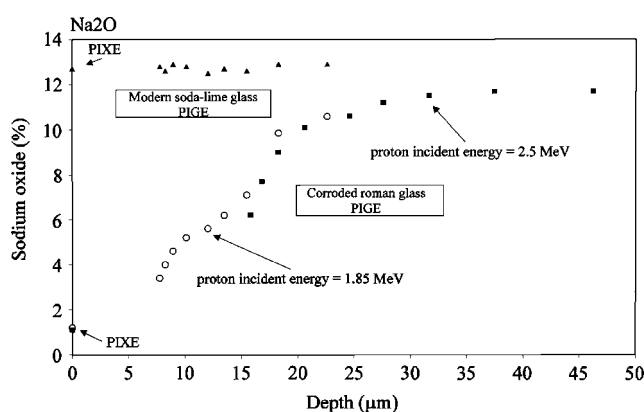


Figure 5. Example of the determination of Na concentration gradient by PIXE/PIGE. Two glasses are concerned: a modern one from Glaverbel and a Roman one from the Curtius Museum in Liège, Belgium.

were used and it is worth noting that the two specific curves are well connected. The values of Na concentration at a  $0^\circ$  angle correspond for the two energies to the data obtained by PIXE under a helium atmosphere. They consist of the concentration at the near surface because the Na x-rays (1.04 keV) induced in depth are unable to reach the detector. It should be noted that the measurements performed on modern glass (soda-lime glass) give a result corresponding to a homogeneous distribution of Na in the bulk. It proves that there is no migration of the Na ions in the glass network under particle bombardment.

Concerning the general accuracy of the method, the problem of the statistical error is negligible because of the large counting rate obtained with PIGE. The main error source is the surface quality, which can increase the slowing of the proton differential. Fortunately, the relatively large beam spot (1 mm in diameter) smooths this effect and allows an averaged result that is macroscopically representative. On glass with a reasonably flat surfaces lightly larger than the beam spot, the precision is better than 10%. This was checked on samples of blowing glass manufactured according to the ancient technique, different from the modern float process.

We checked the present technique by using the confocal Raman technique on the same Roman glass sample. This

method showed that the Raman spectrum became that of the normal soda-lime glass only about 25  $\mu\text{m}$  below the glass surface. This corresponds well, on Fig. 5, to the depth where the Na concentration becomes stable.

## CONCLUSIONS

The method described in this paper is important in the field of archaeometry because of its non-destructive aspect. However, whereas qualitative information is relatively accessible, quantitative data depend strongly of the knowledge of several parameters such as reaction and x-ray production cross-sections, composition of the medium, binders, glass, etc. in major elements which determine the charged particle stopping power and the x-ray absorption coefficients. The writing of specific computing programs allowing the a maximum amount of these data to be taken into account will be a major improvement in the future.

## Acknowledgments

We are indebted to the Institut Universitaire des Sciences Nucléaires and the French Belgian Community (ARC) for their financial support.

## REFERENCES

1. Grime W, Watt F. *Nucl. Instrum. Methods B* 1993; **75**: 495.
2. Swann CP. *Nucl. Instrum. Methods B* 1995; **104**: 576.
3. Absil J, Garnir HP, Strivay D, Oger C, Weber G. *Nucl. Instrum. Methods B* 2002; **189**: 350.
4. Weber G, Delbrouck JM, Strivay D, Kerff F, Martinot L. *Nucl. Instrum. Methods B* 1998; **139**: 196.
5. Weber G, Strivay D, Martinot L, Garnir HP. *Nucl. Instrum. Methods B* 2002; **189**: 350.
6. Jembrish-Simbürger D, Neelmeijer C, Schalm O, Fredricks P, Schreiner M, de Vis K, Mäder M, Caen J. *J. Anal. At. Spectrom.* 2002; **17**: 321.
7. Ziegler JF, Biersack JP. *SRIM 2000.39 Software*. IBM Research: USA, 2000.
8. Berger MJ. *X-com Software* 12. 1987.
9. Paul H. *Nucl. Instrum. Methods B* 1984; **3**: 5.
10. Strivay D, Weber G. *Nucl. Instrum. Methods B* 2002; **1190**: 112.
11. Feller RL. *Artists' Pigments: Handbook*, vol. 1. Oxford University Press: Oxford, 1985; 169.
12. Bomford D, Dunkerton J, Gordon D, Roy A. *Italian Painting Before 1400*. National Gallery: London, 1989; 42.
13. Puraye J. *Rev. Belge Archéol. Hist. Art.* 1939; **3**: 193.
14. Bodard F, Deconninck G, Demortier G. *J. Radioanal. Chem.* 1977; **35**: 95.